A Double-walled Noncovalent Carbon Nanotube by Columnar Packing of Nanotube Fragments

Daiki Imoto[†], Hiroki Shudo[†], Akiko Yagi*[,†,‡], and Kenichiro Itami*[,‡,°]

[†] Department of Chemistry, Graduate School of Science, Nagoya University, Nagoya 464-8602, Japan.

[‡] Institute of Transformative Bio-Molecules (WPI-ITbM), Nagoya University, Nagoya 464-8602, Japan.

[°] Molecule Creation Laboratory, RIKEN Cluster for Pioneering Research, RIKEN, Wako, Saitama 351-0198, Japan.

KEYWORDS: Nanobelt, Perfluorocycloparaphenylene, Noncovalent nanotube, Crystal engineering

ABSTRACT: Double-walled nanotubes are promising materials in various scientific fields because of their high stability and large surface area. Herein, we report the synthesis of double-walled noncovalent carbon nanotubes (CNTs) through host–guest complexation of nanotube fragments and tube-forming crystal engineering. As the smallest fragment of double-walled CNTs, a host–guest complex of perfluorocycloparaphenylene (PFCPP) and carbon nanobelt (CNB) was synthesized by mixing them in solvents. The immediate complexation of the PF[12]CPP⊃(6,6)CNB complex with a remarkably high association constant (K_a) of 2×10^5 L/mol was observed. Time-dependent ^{1}H NMR and thermogravimetry measurements revealed that the stability of (6,6)CNB was significantly improved by encapsulation. X-ray crystallography confirmed the robust belt-in-ring structure of this complex. As indicated by the short distance between PF[12]CPP and (6,6)CNB (2.8 Å), intermolecular orbital interactions exist between the belt and the ring, which were further supported by theoretical calculation and phosphorescence quenching experiments. While the PF[12]CPP⊃(6,6)CNB complex adopts various crystal packing structures, chloroform was discovered to be a magic "glue" solvent inducing one-dimensional alignment of the PF[12]CPP⊃(6,6)CNB complex to build an unprecedented double-walled noncovalent CNT structure.

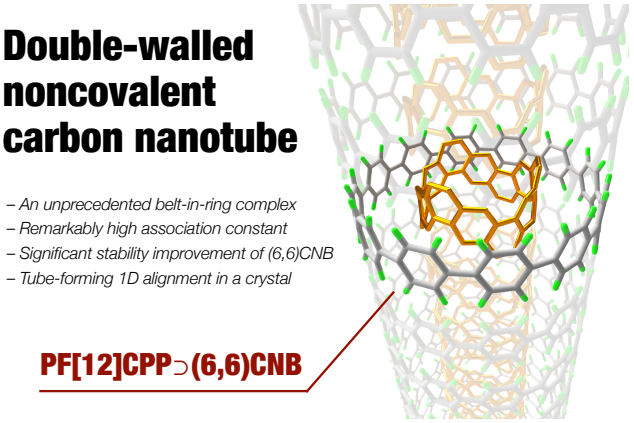

INTRODUCTION

Carbon nanotubes (CNTs) have hollow tube-like cylindrical structure.[1] Double-walled CNTs consist of two coaxial layers of nanotubes that are known to be thermally and chemically more stable than single-walled CNTs and more flexible than multi-walled CNTs (Figure 1A).[2-6] However, current methods for synthesizing double-walled CNTs cannot precisely control the diameter and helicity of the CNTs, resulting in the physical properties of the CNTs being an average of the mixture. Therefore, the controlled synthesis of double-walled CNTs is required to induce defined macroscopic material properties. Cycloparaphenylenes (CPPs) and carbon nanobelts (CNBs) have been synthesized as armchair-type CNT fragments.[7-12] Since these host–guest complexes of CNT fragments can be regarded as ultrashort double-walled CNTs, the synthesis and property evaluation of such host–guest complexes have also been explored in recent years.[13-15] These host–guest complexes can serve as a potential platform for bottom-up synthesis of molecularly defined double-walled CNTs.

A possible route for synthesizing molecularly defined double-walled CNTs is to convert noncovalent nanotubes, in which each fragment, such as CPP and CNB, is flexibly bound by noncovalent interactions, into double-walled CNTs (Figure 1A). However, it has been well established that most CPPs and CNBs arrange themselves in a herringbone packing arrangement via intermolecular CH–π interactions, making it challenging to achieve the synthesis of noncovalent CNTs via one-dimensional (1D) assembly of CNT fragments.[10,12] In contrast, certain substituted CPPs are known to assemble in a 1D manner by preventing CH–π interactions through the introduction of substituents or by incorporating strong interactions such as hydrogen bonds.[16-20] Therefore, we hypothesized that 1D alignment of double-walled CNT fragments could be accomplished by carefully designed host–guest complexes with substituted CPPs (Figure 1A). Such double-walled noncovalent CNTs represent a novel nanomaterial that combines the diverse chemical properties of noncovalent supramolecular nanotubes,[21-24] with the structural rigidity of CNTs. Once the host–guest complex is assembled in a 1D manner in the crystal, the precise construction of double-walled noncovalent nanotubes at the molecular level can be confirmed by

X-ray structural analysis. Herein, we report the synthesis of double-walled noncovalent CNTs through very strong host–guest complexation of perfluoro[12]CPP (PF[12]CPP)[19] and (6,6)carbon nanobelt ((6,6)CNB)[11], followed by tube-forming crystal engineering (Figure 1B). Density functional theory (DFT) calculations and phosphorescence measurements suggest that this host–guest complex has intramolecular orbital interactions. While the PF[12]CPP⊃(6,6)CNB complex adopts various crystal packing structures, chloroform was discovered to be a magic "glue" solvent inducing 1D alignment of PF[12]CPP⊃(6,6)CNB to build an unprecedented double-walled noncovalent CNT structure.

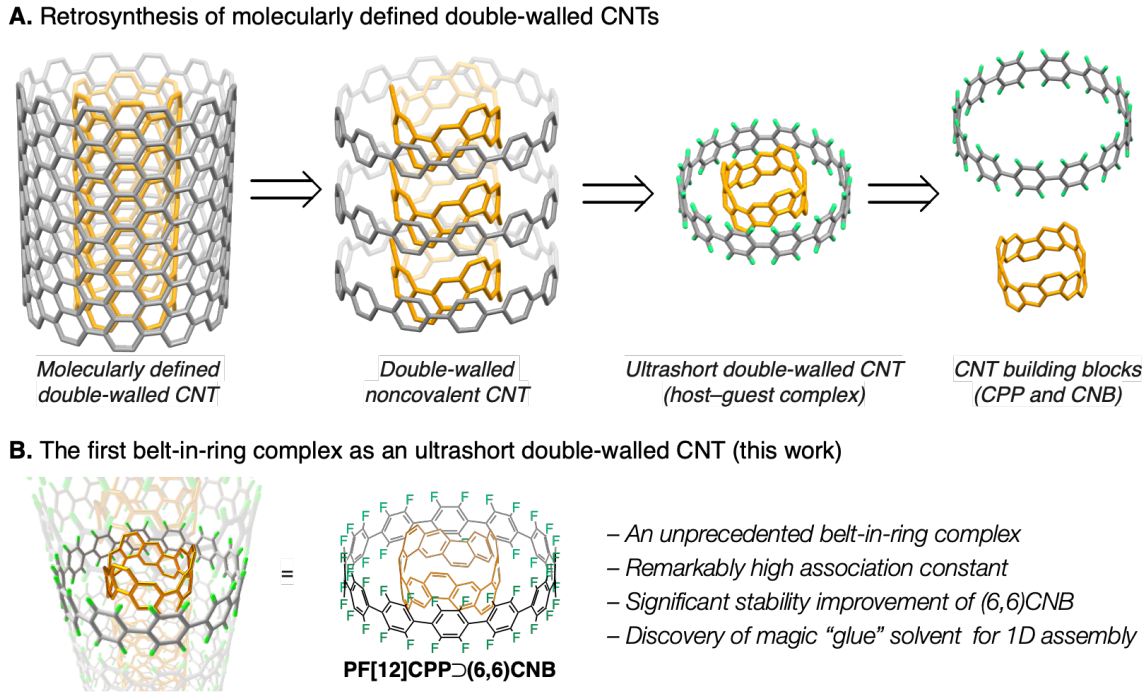

Figure 1. (A) Retrosynthesis of molecularly defined double-walled CNTs. (B) The first belt-in-ring complex as an ultrashort double-walled CNT (this work).

RESULTS AND DISCUSSION

Design of double-walled noncovalent carbon nanotubes

We believe that there are four essential conditions for the conversion of a double-walled noncovalent CNT into a molecularly defined double-walled CNT (Figure 1). First, the double-walled noncovalent CNTs must have ultrashort double-walled CNTs as components containing all the necessary carbon atoms in the double-walled CNTs (condition 1). Double-walled noncovalent CNTs must be capable of being converted into double-walled CNTs by linking the components through C–C bond formation. Additionally, these ultrashort double-walled CNTs must be able to form nanotubes through 1D assembly (condition 2). Furthermore, the host–guest complexes should have high stability and association constants to endure the conditions of component-assembling C–C bond formation (condition 3). Lastly, for successful tubular assembly, "glue" molecules are required to fill the internal space of the host–guest complex and link the complexes together to help achieve otherwise-difficult 1D alignment (condition 4).

Perfluorocycloparaphenylenes (PFCPPs) have a structure in which all the hydrogen atoms of CPPs are replaced by fluorine atoms.[19] Unlike pristine CPPs, PFCPPs are known to adopt columnar packing through van der Waals interactions in various ring sizes because PFCPPs lack C–H bonds that would trigger the formation of various crystal packings through CH–π interactions. Therefore, we envisioned that host–guest complexes with PFCPP components would help the host–guest complexes to be arranged in a 1D assembly in crystals. There are two possible approaches for utilizing PFCPP: either as a host or as a guest molecule. If PFCPP is used as a guest molecule, CH–π interactions between the host molecules such as CPP or CNB would prevent 1D packing. Conversely, the use of PFCPP as a host molecule allows for 1D packing while providing a tubular internal space. By arranging guest molecules in this internal space, CH–π interactions between guest molecules are inhibited from forming double-walled noncovalent CNTs. As a guest molecule, CNBs were chosen considering their higher rigidity compared to CPPs and their reduced tendency to form unexpected arrangements due to CH–π interactions between guest molecules. In addition, we expected that a donor–acceptor-type interaction between CNB and PFCPP might occur to help constructing a strong host–guest complex. Thus, we began by computational screening regarding the combination of complex partners by DFT calculations that led to the suggestion that PF[12]CPP is the best candidate for encapsulating (6,6)CNB (see Figure S11 in Supporting Information (SI)).

Synthesis of PF[12]CPP⊃(6,6)CNB and NMR analysis

The synthesis of host–guest complexes of PF[12]CPP and (6,6)CNB is extremely simple and facile. One equivalent of (6,6)CNB was mixed with PF[12]CPP in CH_2Cl_2 and PF[12]CPP⊃(6,6)CNB was obtained by heating the mixed solution in air at 40 °C for 5 min (Figure 2A). The structural properties

of PF[12]CPP⊃(6,6)CNB were investigated by ^{1}H NMR analysis (Figure 2B). In CD_2Cl_2, the ^{1}H NMR spectrum of pristine (6,6)CNB shows two singlet signals at 8.32 ppm and 7.54 ppm. In contrast, the ^{1}H NMR spectrum of PF[12]CPP⊃(6,6)CNB exhibits two singlet signals at 7.57 ppm and 7.09 ppm. Based on previously reported assignments and ^{1}H NMR prediction with DFT calculation of (6,6)CNB,[11] the signal observed at 7.57 ppm can be assigned to hydrogen atoms in the *K*-region, while the signal observed at 7.09 ppm can be assigned to hydrogen atoms in the *bay*-region of (6,6)CNB. Therefore, it is likely that the signals in the *K*- and *bay*-regions shift toward a higher magnetic field when encapsulation within PF[12]CPP takes place. Moreover, when adding two equivalents of (6,6)CNB to PF[12]CPP in a CD_2Cl_2 solution, the signals of free (6,6)CNB and of PF[12]CPP⊃(6,6)CNB were observed simultaneously. This result indicates that PF[12]CPP⊃(6,6)CNB has slower association and dissociation processes compared to the ^{1}H NMR relaxation time. This shift in each signal can be attributed to the shielding effect of the host PF[12]CPP molecule. Consequently, the effect of solvent on ^{1}H NMR spectra was investigated. In $CDCl_3$ and CD_2Cl_2, the signals of (6,6)CNB were also shifted whereas no signals were shifted in DMSO-d_6, clearly showing that the formation of PF[12]CPP⊃(6,6)CNB is a solvent-dependent process (see Figure S13 in SI). The association constant (K_a) of the host–guest complex was determined by the integral ratio of the ^{1}H NMR spectrum in a mixed solvent of $CDCl_3$ and CS_2 (v/v = 4:3).

$$K_a = \frac{[\text{PF[12]CPP} \supset (6,6)\text{CNB}]}{[\text{PF[12]CPP}][(6,6)\text{CNB}]}$$

Using the above equation, K_a was determined to be 2×10^5 L/mol (Figure 2C). Compared to the K_a values of [*n*+5]CPP⊃[*n*]CPP in 1,1,2,2-tetrachloroethane-d_2 solution at 50 °C ($K_a < 10^3$ L/mol) reported by Yamago *et al.*,[13] PF[12]CPP⊃(6,6)CNB has a remarkably large K_a value. This high K_a is likely due to the entropy effect caused by expulsion of the encapsulated solvent and weak orbital interactions between PF[12]CPP and (6,6)CNB. Notably, during the NMR experiments conducted under air in solution, (6,6)CNB remained nearly unchanged. This is in sharp contrast to pristine (6,6)CNB, which undergoes decomposition under air in solution. A significant increase in the stability of (6,6)CNB against oxidation is thought to occur because the sidewall of (6,6)CNB is covered by PF[12]CPP to block reactions with oxygen (see Figure S14 and S15 in SI). Thermogravimetry (TG) measurements were also conducted to investigate the thermal stability of PF[12]CPP, (6,6)CNB and PF[12]CPP⊃(6,6)CNB (see Figure S10 in SI). These results indicate that the thermal decomposition behavior is changed by encapsulation, and clearly show that the stability of PF[12]CPP⊃(6,6)CNB against heat is also significantly improved from that of (6,6)CNB. Furthermore, the signal of the host–guest complex was even detected in the MALDI-TOF MS spectrum (see Figure S20 in SI).

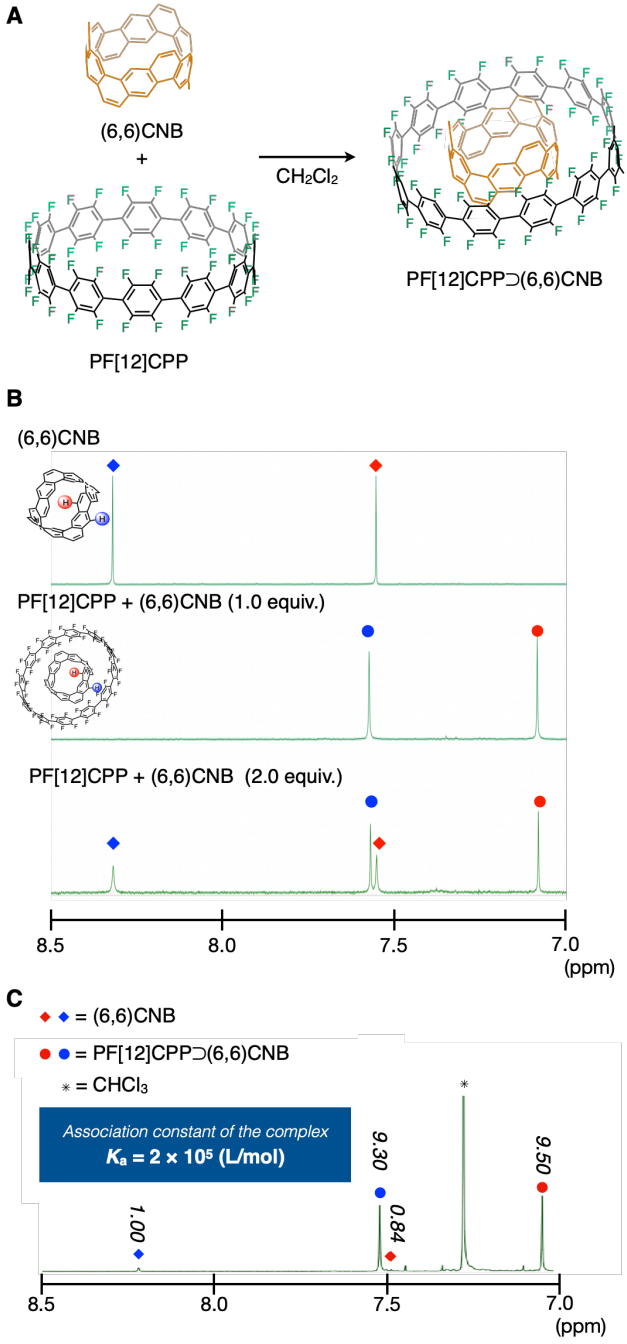

Figure 2. (A) Synthesis of PF[12]CPP⊃(6,6)CNB: (6,6)CNB (1.0 equiv.), PF[12]CPP (1.0 equiv.), CH_2Cl_2, under air, room temperature. (B) ^{1}H NMR spectra of CD_2Cl_2 solution of (6,6)CNB, PF[12]CPP+(6,6)CNB (1.0 equiv.), and PF[12]CPP+(6,6)CNB (2.0 equiv.). (C) ^{1}H NMR spectra of PF[12]CPP⊃(6,6)CNB to determine association constant in a mixed solvent of $CDCl_3$ and CS_2 (v/v = 4:3). The vertical numbers in ^{1}H NMR spectrum represent the integral ratio of each signal.

Photophysical properties of PF[12]CPP⊃(6,6)CNB

In the optimized structure of PF[12]CPP⊃(6,6)CNB, the distance between the host molecule and the guest molecule is approximately 2.8 Å, which is close enough to suggest the existence of an intermolecular orbital interaction. Thus, the frontier molecular orbital of PF[12]CPP⊃(6,6)CNB was calculated and illustrated by DFT, which suggested the existence of a weak intermolecular orbital interaction (Figure 3A and 3B). Therefore, the photophysical properties were measured to clarify the orbital interactions. Although no signal change was observed in the absorption or fluorescence spectra (see Figure S7 in SI), low-temperature phosphorescence measurements in 2-MeTHF revealed that the phosphorescence intensity decreased with the addition of (6,6)CNB to PF[12]CPP (Figure 3C). This phosphorescence quenching process is most likely due to the transfer of excitons on PF[12]CPP to (6,6)CNB via intermolecular orbital interactions, leading to a nonradiative deactivation pathway.

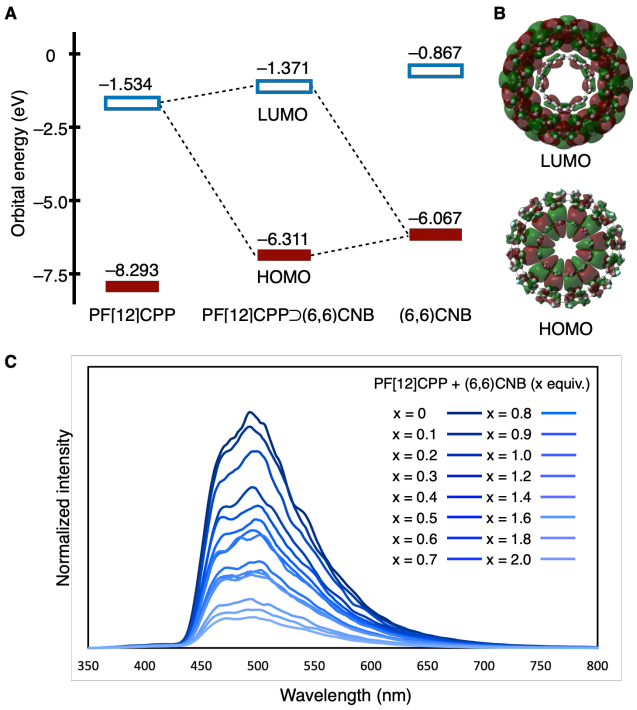

Figure 3. (A) Frontier molecular orbital energy of (6,6)CNB, PF[12]CPP, and PF[12]CPP⊃(6,6)CNB. (B) Isosurface of PF[12]CPP⊃(6,6)CNB (calculated by the CAM-B3LYP/6-31G(d) level of theory, isovalue = 0.001). (C) Phosphorescence spectra change of PF[12]CPP by adding (6,6)CNB in 2-MeTHF at 77 K (excitation at 270 nm).

Construction of noncovalent nanotubes

The molecular and packing structures of PF[12]CPP⊃(6,6)CNB were successfully determined by X-ray crystallography.[25] Single crystals of PF[12]CPP⊃(6,6)CNB were obtained from chloroform/pentane solution. This crystal structure showed a "dimeric" brickwall packing structure (Figure 4A; see also Figures S1 and S2 in SI). The observation of noncolumnar packing structure of PF[12]CPP⊃(6,6)CNB was initially somewhat disappointing, but the careful examination led to the analysis that this unique packing is due to the encapsulated pentane, preventing the formation of a columnar packing structure with more than three molecules. This analysis suggests that encapsulated solvent can dictate the packing structure of PF[12]CPP⊃(6,6)CNB. Previous studies also suggested that the packing mode of pristine CPPs can be adjusted by carefully optimizing the recrystallization conditions.[26,27] To manipulate the packing structure, the solvent used in the crystallization process was modified. When 1,1,1-trichloroethane was used as the good solvent and octane was used as the poor solvent, the crystals showed a herringbone assembly (Figure 4B; see also Figures S3 and S4 in SI). This is possibly because the encapsulated octane molecule protrudes on both sides of PF[12]CPP⊃(6,6)CNB, preventing columnar assembly. Therefore, encapsulated solvents that are smaller in size than PF[12]CPP⊃(6,6)CNB and do not interfere with columnar packing are considered to work as "glue" molecules that link the host–guest complex together to form a 1D assembly.

Our investigation along this line led to the discovery that chloroform was discovered to be a magic "glue" solvent inducing 1D alignment of the host–guest complex. Needle-shaped crystals of PF[12]CPP⊃(6,6)CNB were obtained by slow evaporation of chloroform solution (Figure 4C; see also Figures S5 and S6 in SI). In the crystal structure, PF[12]CPP⊃(6,6)CNB aligns with columns to form double-walled noncovalent CNT. Chloroform is located between the two molecules of PF[12]CPP⊃(6,6)CNB in the crystal (Figure 4D). This chloroform acts as a "glue" solvent, inducing a 1D alignment of PF[12]CPP⊃(6,6)CNB to build a double-walled noncovalent CNT. In addition, slight disorder is observed both above and below the (6,6)CNB in this crystal. This disorder suggests that (6,6)CNB exists within the PF[12]CPP cavity with some dispersion (Figure 4E). By conducting Hirshfeld surface analysis of the double-walled noncovalent nanotubes using (6,6)CNB as a probe, the surface of the host–guest complex was further inspected (Figure 4F). This surface analysis revealed that the (6,6)CNB in the upper and lower complexes were sufficiently close to each other. These results also indicate that the construction of novel double-walled noncovalent CNTs were achieved by the precise arrangement of (6,6)CNB in the crystal.

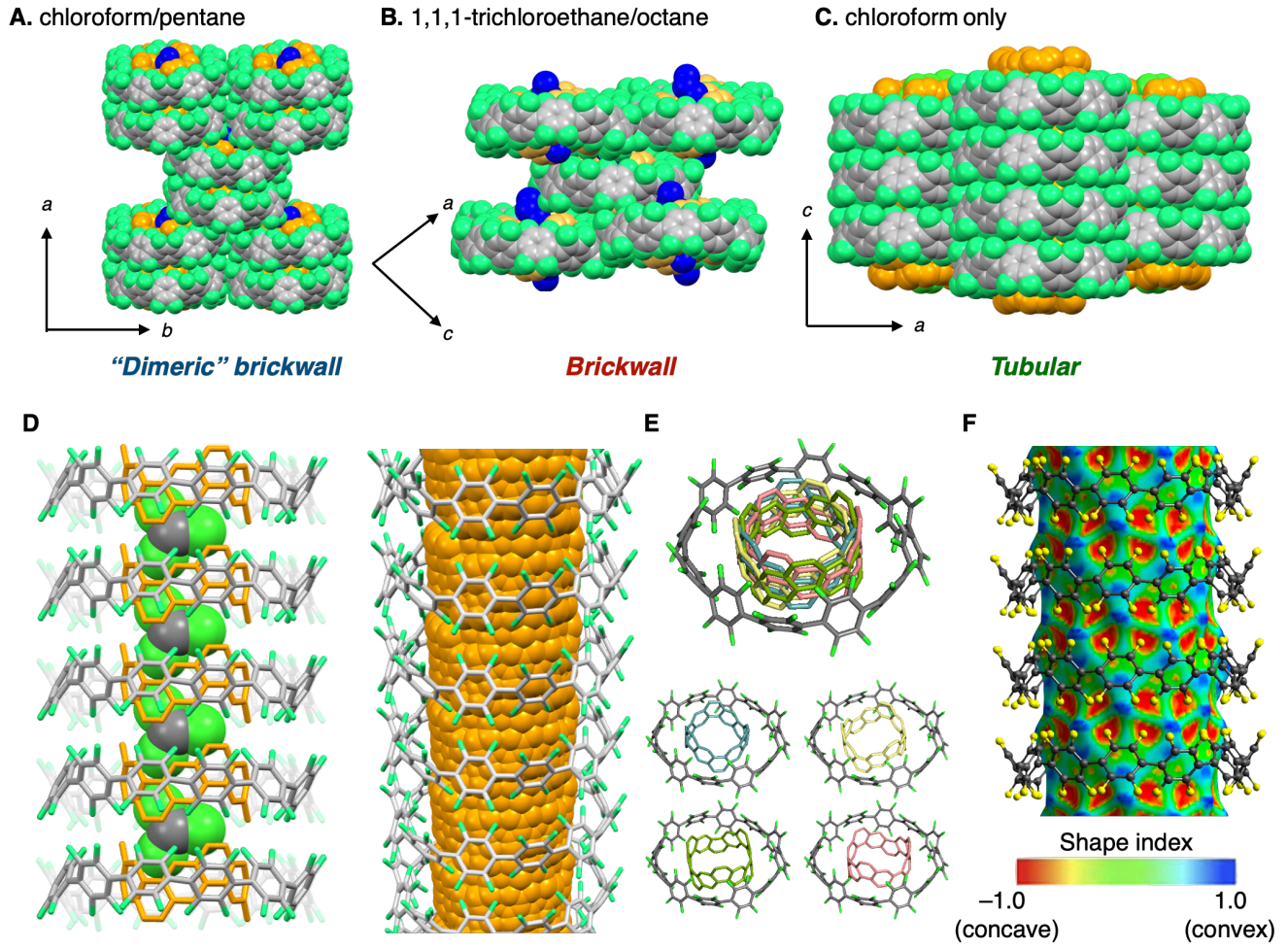

Figure 4. ORTEP and packing structures of PF[12]CPP⊃(6,6)CNB from chloroform/pentane (A), 1,1,1-trichloroethane/octane (B), and chloroform. (C) with thermal ellipsoids at 50% probability (hydrogen atoms and some solvents are omitted for clarity). PF[12]CPP are represented in gray and green, (6,6)CNB are represented in orange, and solvent are represented in blue. (D) Magic "glue" solvent effect inducing 1D alignment of PF[12]CPP⊃(6,6)CNB to build a double-walled noncovalent CNT. (E) Crystal structure of PF[12]CPP⊃(6,6)CNB and its disorders. Four different orientations of (6,6)CNB were shown in different colors. (F) Hirshfeld surface analysis of double-walled noncovalent nanotube.

CONCLUSION

In summary, we have synthesized PF[12]CPP⊃(6,6)CNB, which represents the shortest fragment of double-walled noncovalent carbon nanotubes. Formation of the host–guest complex was confirmed by NMR, MALDI-TOF MS, and X-ray crystallography. Time-dependent ^{1}H NMR and thermogravimetry measurements revealed that the stability of (6,6)CNB was significantly improved by encapsulation. While PF[12]CPP⊃(6,6)CNB exhibited a "dimeric" brickwall alignment from chloroform/pentane and brickwall packing from 1,1,1-trichloroethane/octane in crystals, the crystals recrystallized from chloroform adopted a tubular arrangement. These results indicate that the encapsulated solvent molecules dictate the packing structure. This tubular arrangement represents a new class of nanotubes, double-walled noncovalent CNTs, which are expected to be not only promising supramolecular materials[28] with high structural uniformity and structural resilience but also a component for molecularly defined double-walled CNTs.

ASSOCIATED CONTENT

Supporting Information

The Supporting Information is available free of charge on the website at DOI: XXXX.

Experimental procedures, ^{1}H, ^{19}F and ^{13}C NMR spectra, characterization data for all new compounds, optical properties, computational data, and crystallographic data of PF[12]CPP⊃(6,6)CNB (CIF).

AUTHOR INFORMATION

Corresponding Authors

Akiko Yagi – Department of Chemistry, Graduate School of Science and Institute of Transformative Bio-Molecules (WPI-ITbM), Nagoya University, Nagoya 464-8602, Japan; Email: yagi.akiko@itbm.nagoya-u.ac.jp

Kenichiro Itami – Molecule Creation Laboratory, RIKEN Cluster for Pioneering Research, RIKEN, Wako, Saitama 351-0198, Japan.; Email: kenichiro.itami@riken.ac.jp

Authors

Daiki Imoto – Department of Chemistry, Graduate School of Science, Nagoya University, Nagoya 464-8602, Japan.

Hiroki Shudo – Department of Chemistry, Graduate School of Science, Nagoya University, Nagoya 464-8602, Japan.

Author Contributions

The manuscript was written through contributions of all authors.

Funding Sources

This work is supported by JSPS KAKENHI grants (19H05463 to K.I. and 22K21346 to A.Y.) and Sumitomo Foundation (to A.Y.).

ACKNOWLEDGMENT

We thank Prof. Nobuo Kimizuka and Assist. Prof. Kiichi Mizukami (Kyushu University) for a fruitful discussion on this work. We also thank Mr. Tsubasa Okumura for his experimental support. D.I. and H.S. thank the JSPS fellowship for young scientists, Nagoya University Graduate Program of Transformative Chem-Bio Research (WISE program) supported by MEXT, and Nagoya University Interdisciplinary Frontier Fellowship. Fluorescence measurements were conducted using resources from the Chemical Instrumentation Facility, Research Center for Materials Science, Nagoya University. The computations were performed using the Research Center for Computational Science, Okazaki, Japan (Project Nos.:21-IMS-C070 and 22-IMS-C069). The authors declare no competing financial interest.

REFERENCES

1. Iijima, S. Helical microtubules of graphitic carbon. *Nature* **1991**, *354*, 56–58. DOI: 10.1038/354056a0
2. Green, A. A.; Hersam, M. C. Processing and properties of highly enriched double-wall carbon nanotubes. *Nat. Nanotechnol.* **2009**, *4*, 64–70. DOI: 10.1038/nnano.2008.364
3. Endo, M.; Muramatsu, H.; Hayashi, T.; Kim, Y. A.; Terrones, M.; Dresselhaus, M. S. 'Buckypaper' from coaxial nanotubes. *Nature* **2005**, 433, 47. DOI: 10.1038/433476a.
4. Shen, C.; Brozena, A. H.; Wang, Y. Double-walled carbon nanotubes: Challenges and opportunities. *Nanoscale* **2011**, *3*, 503–518. DOI: 10.1039/C0NR00620C
5. Saito, R.; Matsuo, R.; Kimura, T.; Dresselhaus, G.; Dresselhaus, M. S. Anomalous potential barrier of double-wall carbon nanotube. *Chem. Phys. Lett.* **2001**, 348, 187–193. DOI: 10.1016/S0009-2614(01)01127-7
6. Green, A. A.; Hersam, M. C. Properties and Application of Double-Walled Carbon Nanotubes Sorted by Outer-Wall Electronic Type. *ACS Nano* **2011**, 5, 1459–1467. DOI: 10.1021/nn103263b
7. Jasti, R.; Bhattacharjee, J.; Neaton, J. B.; Bertozzi, C. R. Synthesis, Characterization, and Theory of [9]-, [12]-, and [18]Cycloparaphenylene: Carbon Nanohoop Structures. *J. Am. Chem. Soc.* **2008**, *52*, 17646–17647. DOI: 10.1021/ja807126u
8. Takaba, H.; Omachi, H.; Yamamoto, Y.; Bouffard, J.; Itami, K. Selective Synthesis of [12]Cycloparaphenylene. *Angew. Chem., Int. Ed.* **2009**, *48*, 6112–6116. DOI: 10.1002/anie.200902617
9. Yamago, S.; Watanabe, Y.; Iwamoto, T. Synthesis of [8]Cycloparaphenylene from a Square-Shaped Tetranuclear Platinum Complex. *Angew. Chem., Int. Ed.* **2010**, *49*, 757–759. DOI: 10.1002/anie.200905659
10. (a) Lewis, S. E. Cycloparaphenylenes and related nanohoops. *Chem. Soc. Rev.* **2015**, *44*, 2221–2304. DOI: 10.1039/C4CS00366G. (b) Segawa, Y.; Yagi, A.; Matsui, K.; Itami, K. Design and Synthesis of Carbon Nanotube Segments. *Angew. Chem., Int. Ed.* **2016**, *55*, 5136–5158. DOI: 10.1002/anie.201508384. (c) Leonhardt, E. J.; Jasti, R. Emerging applications of carbon nanohoops. *Nat. Rev. Chem.* **2019**, *3*, 672–686. DOI: 10.1038/s41570-019-0140-0. (d) Li, Y.; Kono, H.; Maekawa, T.; Segawa, Y.; Yagi, A.; Itami, K. Chemical Synthesis of Carbon Nanorings and Nanobelts. *Acc. Mater. Res.* **2021**, *2*, 681–691. DOI: 10.1021/accountsmr.1c00105
11. Povie, G.; Segawa, Y.; Nishihara, T.; Miyauchi, Y.; Itami, K. Synthesis of a carbon nanobelt. *Science* **2017**, *356*, 172–175. DOI: 10.1126/science.aam8158
12. Imoto, D.; Yagi, A.; Itami, K. Carbon Nanobelts: Brief History and Perspective. *Precis. Chem.* **2023**, *1*, 516–523. DOI: 10.1021/prechem.3c00083
13. Hashimoto, S.; Iwamoto, T.; Kurachi, D.; Kayahara, E.; Yamago, S. Shortest Double-Walled Carbon Nanotubes Composed of Cycloparaphenylenes. *ChemPlusChem* **2017**, *82*, 1015–1020. DOI: 10.1002/cplu.201700097
14. Zhao, C.; Liu, F.; Feng, L.; Nie, M.; Lu, Y.; Zhang, J.; Wang, C.; Wang, T. Construction of a double-walled carbon nanoring. *Nanoscale* **2021**, *13*, 4880–4886. DOI: 10.1039/D0NR08931A
15. Freiberger, M.; Frühwald, S.; Minameyer, M. B.; Görling, A.; Drewello, T. New Insights into Ring-In-Ring Complexes of [*n*]Cycloparaphenylenes including the [12]Carbon Nanobelt. *J. Phys. Chem. A* **2023**, *127*, 9495–9501. DOI: 10.1021/acs.jpca.3c05644
16. Van Raden, J. M.; Leonhardt, E. J.; Zakharov, L. N.; Pérez-Guardiola, A.; Pérez-Jiménez, A. J.; Marshall, C. R.; Brozek, C. K.; Sancho-García, J. C.; Jasti, R. Precision Nanotube Mimics via Self-Assembly of Programmed Carbon Nanohoops. *J. Org. Chem.* **2020**, *85*, 129–141. DOI: 10.1021/acs.joc.9b02340
17. Hashimoto, S.; Kayahara, E.; Mizuhata, Y.; Tokitoh, N.; Takeuchi, K.; Ozawa, F.; Yamago, S. Synthesis and Physical Properties of Polyfluorinated Cycloparaphenylenes. *Org. Lett.* **2018**, *20*, 5973–5976. DOI: 10.1021/acs.orglett.8b02715
18. Kamin, A. A.; Clayton, T. D.; Otteson, C. E.; Gannon, P. M.; Krajewski, S.; Kaminsky, W.; Jasti, R.; Xiao, D. J. Synthesis and metalation of polycatechol nanohoops derived from fluorocycloparaphenylenes. *Chem. Sci.* **2023**, *14*, 9724–9732. DOI: 10.1039/D3SC03561A
19. Shudo, H.; Kuwayama, M.; Shimasaki, M.; Nishihara, T.; Takeda, Y.; Mitoma, N.; Kuwabara, T.; Yagi, A.; Segawa, Y.; Itami, K. Perfluorocycloparaphenylenes. *Nat. Commun.* **2022**, *13*, 3713. DOI: 10.1038/s41467-022-31530-x
20. Shudo, H.; Kuwayama, M.; Segawa, Y.; Yagi, A.; Itami, K. Half-substituted fluorocycloparaphenylenes with high symmetry: synthesis, properties and derivatization to densely substituted carbon nanorings. *Chem. Commun.* **2023**, *59*, 13494–13497. DOI: 10.1039/D3CC04887J
21. Kameta, N.; Minamikawa, H.; Masuda, M. Supramolecular organic nanotubes: how to utilize the inner nanospace and the outer space. *Soft Matter* **2011**, *7*, 4539–4561. DOI: 10.1039/C0SM01559H
22. Ghadiri, M. R.; Granja, J. R.; Milligan, R. A.; McRee, D. E.; Khazanovich, N. Self-assembling organic nanotubes based on a cyclic peptide architecture. *Nature* **1993**, *366*, 324–327. DOI: 10.1038/366324a0
23. Gong, B.; Shao, Z. Self-Assembling Organic Nanotubes with Precisely Defined, Sub-nanometer Pores: Formation and Mass Transport Characteristics. *Acc. Chem. Res.* **2013**, *46*, 2856–2866. DOI: 10.1021/ar400030e
24. Strauss, M. J.; Evans, A. M.; Roesner, E. K.; Monsky, R. J.; Bardot, M. I.; Dichtel, W. R. Divergent Nanotube Synthesis through Reversible Macrocycle Assembly. *Acc. Mater. Res.* **2022**, *3*, 935–947. DOI: 10.1021/accountsmr.2c00062
25. CCDC numbers: 2371687, 2371688 and 2371689.
26. Fukushima, T.; Sakamoto, H.; Tanaka, K.; Hijikata, Y.; Irle, S.; Itami, K. Polymorphism of [6]Cycloparaphenylene for Packing Structure-dependent Host–Guest Interaction. *Chem. Lett.* **2017**, *46*, 855–857. DOI: 10.1246/cl.170210
27. Ozaki, N.; Sakamoto, H.; Nishihara, T.; Fujimori, T.; Hijikata, Y.; Kimura, R.; Irle, S.; Itami, K. Electrically Activated Conductivity and White Light Emission of a Hydrocarbon Nanoring–Iodine Assembly.

Angew. Chem., Int. Ed. **2017**, *56*, 11196–11202. DOI: 10.1002/anie.201703648
28. Dey, K.; Koner, K.; Mukhopadhyay, R. D.; Shetty, D.; Banerjee, R. Porous Organic Nanotubes: Chemistry of One-Dimensional Space. *Acc. Chem. Res.* **2024**, *57*, 1839–1850. DOI: 10.1021/acs.accounts.4c00224

Insert Table of Contents artwork here